

Effective Diffusion Coefficients for Methanol in Sulfuric Acid Solutions Measured by Raman Spectroscopy

Lisa L. Van Loon,[†] Heather C. Allen,^{*,†} and Barbara E. Wyslouzil^{*,†,‡}

Department of Chemistry, The Ohio State University, 100 West 18th Avenue, Columbus, Ohio 43210, and Department of Chemical and Biomolecular Engineering, The Ohio State University, 140 West 19th Avenue, Columbus, Ohio, 43210

Received: June 17, 2008; Revised Manuscript Received: August 17, 2008

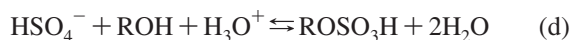
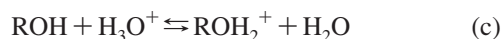
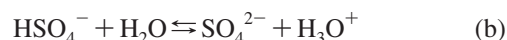
The diffusion of methanol into 0–96.5 wt % sulfuric acid solutions was followed using Raman spectroscopy. Because methanol reacts to form protonated methanol (CH_3OH_2^+) and methyl hydrogen sulfate in H_2SO_4 solutions, the reported diffusion coefficients, D , are effective diffusion coefficients that include all of the methyl species diffusing into H_2SO_4 . The method was first verified by measuring D for methanol into water. The value obtained here, $D = (1.4 \pm 0.6) \times 10^{-5} \text{ cm}^2/\text{s}$, agrees well with values found in the literature. The values of D in 39.2–96.5 wt % H_2SO_4 range from $(0.11\text{--}0.3) \times 10^{-5} \text{ cm}^2/\text{s}$, with the maximum value of D occurring for 61.6 wt % H_2SO_4 . The effective diffusion coefficients do not vary systematically with the viscosity of the solutions, suggesting that the speciation of both methanol and sulfuric acid may be important in determining these transport coefficients.

Introduction

The diffusion of volatile species into atmospheric aerosols containing sulfuric acid is an important step in atmospheric chemical processing that directly affects aerosol scavenging.¹ Sulfuric acid is the predominant aerosol component in the free troposphere,² and H_2SO_4 concentrations of 10^4 to 10^7 molecules cm^{-3} have been measured in the upper troposphere.³

Recent field measurements show that aerosols and cloud droplets can also contain significant amounts of organic compounds,^{4–6} some of which are neutral alcohol species.⁵ In particular, large concentrations of methanol have been detected in both remote and urban regions.^{7–11} These volatile organic compounds are more likely to condense on pre-existing particles than to nucleate new ones, contributing to the growth of these particles.^{12,13}

Currently, there are few measured diffusion coefficients for species of atmospheric importance into sulfuric acid solutions^{1,14,15} and none for the alcohols. The diffusion of an alcohol into sulfuric acid is complicated by the reactions that occur to form secondary compounds.¹⁶ In particular, reactions a–f indicate that, in the presence of sulfuric acid, alcohols may be protonated and react to form sulfate esters.



Although the neutral alcohol and the reaction products are expected to have different diffusion coefficients, by focusing on the diffusion of a common functional group, an overall or effective diffusion coefficient can still be measured.

In this article, we present the effective diffusion coefficients measured for methanol in 0–96.5 wt % sulfuric acid solutions that were obtained by conducting Raman spectroscopy experiments. Bardow et al.¹⁷ recently used position-resolved Raman scattering measurements to determine composition-dependent binary diffusion coefficients in the well-characterized ethyl acetate–cyclohexane system. Our experiments and analysis method are less sophisticated than those of Bardow et al.,¹⁷ due in part the complexity of these reacting mixtures. Thus, we consider this study to be a first step in understanding diffusion processes in complex alcohol– H_2SO_4 systems. Given the paucity of available data, and the difficulty of accurately predicting liquid diffusion coefficients, these measurements should still prove useful to the atmospheric chemistry community and help assess the reliability of commonly used estimation methods for diffusion coefficients.

Our measurements were made by continually flowing a methanol vapor/ $\text{N}_2(\text{g})$ carrier gas mixture over a given solution to maintain a constant surface concentration and observing the appearance of the methanol species at a fixed depth below the surface. The reliability of the method was confirmed by first measuring the diffusion coefficient of methanol into water and comparing the result with values found in the literature. While the experiments presented here are performed at 295 K, the experimental design lends itself to operation at colder temperatures and measuring diffusion coefficients under upper tropospheric conditions may be possible.

Experimental Section

Chemicals. Methanol (HPLC grade, Fisher Scientific), sulfuric acid (redistilled, 96.5 wt %, GFS), and nitrogen gas (N.F. standard) were used as received. Deionized water was obtained from a Millipore Nanopure system (18.1–18.2 M Ω cm).

* To whom correspondence should be addressed. E-mail: wyslouzil.1@osu.edu; allen@chemistry.ohio-state.edu.

[†] Department of Chemistry.

[‡] Department of Chemical and Biomolecular Engineering.

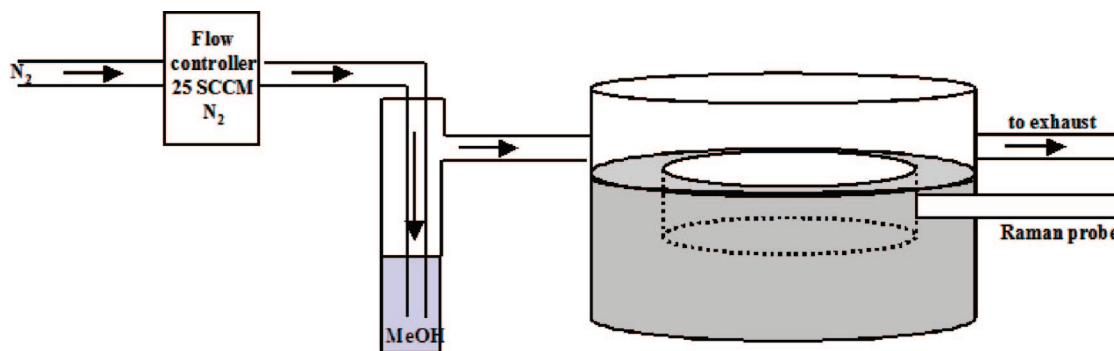


Figure 1. Experimental setup used for Raman experiments.

The H₂SO₄ solutions were prepared by diluting 96.5 wt % H₂SO₄ with deionized water and determining the concentrations by titration to ± 0.1 wt % with a standardized sodium hydroxide solution. The concentrations used in the Raman diffusion experiments were 96.5 wt %, (79.3 ± 0.3) wt %, (61.6 ± 0.1) wt %, and (39.2 ± 0.1) wt %.

A Thermo Nicolet FTIR spectrometer (Avatar 370, Thermo Electron Corporation) measured the concentration of gas-phase methanol using the absorbance of the $\nu_{\text{CO-ss}}$ at 1052 cm^{-1} .^{18,19} The N₂/CH₃OH mixture flowed into an open-ended cell placed in the FTIR sample compartment, and spectra were collected with a spectral resolution of 4 cm^{-1} and 200 scans.

Experimental Setup and Procedures. The experimental setup used is shown in Figure 1. A Petri dish, 1.5-cm deep with a surface area of 19.6 cm^2 , was filled to a depth of 1.2 cm with the appropriate solution and placed inside the flow cell. The N₂/CH₃OH mixture was produced by bubbling nitrogen through methanol at a constant flow rate (Mass Flow Controller 1479A51CS1BM, powered by PRF4000-F2VIN, MKS Instruments). FTIR measurements showed that the methanol concentration in the N₂ increased linearly with the carrier gas flow rate. At a flow rate of 25 SCCM, for example, the CH₃OH concentration was $(1.3 \pm 0.1) \times 10^{17}$ molecules/cm³, whereas at 100 SCCM it was $(4.8 \pm 0.1) \times 10^{17}$ molecules/cm³.

The N₂/CH₃OH mixture enters the cell through the sidewall at a height of 5 cm above the solution surface and exits through an outlet on the opposite side of the cell. As the methanol vapor passes over the solution, it is adsorbed onto the surface and diffuses into the solution. We previously investigated the uptake of methanol at the surface of sulfuric acid solutions by sum frequency generation spectroscopy²⁰ and found that the CH₃OH surface coverage reaches steady state within 15 min of starting the CH₃OH/N₂ flow. By flowing methanol into the cell during the entire experiment, the surface concentration remains constant. We also conducted experiments using different N₂ flow rates (25–100 SCCM) to confirm that the liquid-phase diffusion was independent of the changes in the gas flow rate and concentration and, thus, that gas-phase diffusion was not limiting the diffusion of CH₃OH into the solutions (data not shown). The experiments presented in this work were conducted with an N₂ flow rate of 25 SCCM.

To determine the liquid-phase concentration of the diffusing species, a Raman probe was inserted in the side of the cell and rested against the wall of the dish. By rotating the probe in its holder, the probe depth could be varied between 0.15 and 0.85 cm below the surface. Most of the experiments were conducted at a probe depth of 0.35 cm.

Raman spectra were obtained using 150 mW from a 785-nm continuous wave laser (Raman Systems, Inc.) The backscattered light was collected by a fiber optic probe (InPhotonics) coupled

to the entrance slit of a 500-mm monochromator (Acton Research, SpectraPro 500i), using a 600 groove/mm grating blazed at $1 \mu\text{m}$. The slit width was set at $50 \mu\text{m}$, and the band-pass was 4 cm^{-1} for the H₂SO₄ solution experiments. The slit width was set at $100 \mu\text{m}$, and the band-pass was 5.5 cm^{-1} for the water experiments.

Ideally, the peak used in the analysis does not have interference from solvent peaks. To minimize the error in the measured peak area, the most intense peak with the least solvent interference was used for analysis. In this work, peaks that had minimal overlap with sulfate vibrational modes were used to follow the concentration of methanol (and its reaction products). In particular, the diffusion of CH₃OH into water was monitored using the C–O symmetric stretch present at 1020 cm^{-1} and also with the CH₃ symmetric and asymmetric stretches at 2850 and 2955 cm^{-1} , respectively. Because of the overlapping of H₂SO₄ vibrational modes with the CO stretch of reacted CH₃OH, the diffusion of CH₃OH into 39.2 to 79.3 wt % sulfuric acid solutions was monitored using the CH₃ stretching region (2800 and 3200 cm^{-1}). The diffusion of CH₃OH into 96.5 wt % H₂SO₄ was monitored using the O–S–O symmetric stretch present at 800 cm^{-1} since the CH₃OH is converted to methyl hydrogen sulfate (MHS) on timescales much shorter than the diffusion time.²⁰

In the diffusion experiments, spectra were collected as the average of three 30-s exposures every 10 min for several hours with a liquid nitrogen-cooled CCD camera (Roper Scientific, LN400EB, 1340×400 pixel array, back-illuminated and deep depletion CCD). The electronically controlled laser shutter (Princeton Instruments, ST-133 Controller) only opened when collecting spectra to prevent heating the sample. For each set of experiments, the CCD camera was calibrated using the 435.833-nm line from a fluorescent lamp and by measuring the spectrum of crystalline naphthalene and comparing the experimental peak positions with the accepted literature values.²¹ The CH₃OH–water and the CH₃OH–H₂SO₄ diffusion experiments were conducted at 22 ± 1 and 23 ± 2 °C, respectively.

Spectra were fit using the software package IgorPro 4.05. To determine the peak areas, the spectra were fit with Voigt line shapes using the IgorPro multipeak fitting function with the baseline subtraction enabled. Care was taken to keep the Voigt shape constant for a given peak by fitting the most intense spectrum and then applying that Voigt shape when fitting the other spectra.

Data Analysis. In a one-dimensional diffusion experiment, when there is no variation in the diffusion coefficient or the solution density, Fick's second law, eq 1, relates the change in concentration, c , as a function of time, t , to the second derivative in concentration, $\partial^2 c / \partial z^2$ through the diffusion coefficient D (cm^2/s)

$$\frac{\partial c}{\partial t} = D \frac{\partial^2 c}{\partial z^2} \quad (1)$$

In our experiments, the spatial variable z is the distance from the surface of the solution, the initial condition is pure solvent, and the boundary conditions include a constant concentration of methanol at the liquid–vapor interface ($z = 0$) and zero mass flux at the bottom ($z = L$) of the dish.²² That is,

$$\text{at } t = 0, c = 0 \text{ for } 0 < z < L$$

$$\text{at } t > 0, c = c_0 \text{ for } z = 0$$

$$\text{and } \partial c / \partial z = 0 \text{ at } z = L$$

Under these conditions, the solution to eq 1 is given by^{22,23}

$$c(z, t) = c_0 \left\{ 1 - \frac{4}{\pi} \sum_{\nu=0}^{\nu=\infty} \frac{1}{2\nu+1} \sin \frac{(2\nu+1)\pi z}{2L} \times \exp \left[- \left(\frac{(2\nu+1)\pi}{2L} \right)^2 D t \right] \right\} \quad (2)$$

In eq 2, $c(z, t)$ is the concentration (molecules/cm³), c_0 is the constant concentration at the solution surface, ν is an integer, and L is the solution thickness (cm). D is assumed to be independent of concentration, and this assumption is valid if the change in the diffusion coefficient is minimal for the increase in solution concentration during the measurement.^{22,24} Raman spectroscopy can be used as a quantitative method after careful consideration of transition moment strength. From our calibration curves (Supporting Information), there is a linear relationship between the solute concentration and the measured peak area. To determine the diffusion coefficient, it is, therefore, equally valid to simply fit the peak areas after adjusting these for any nonzero intercept observed in the calibration. Thus, we used IgorPro to do a weighted nonlinear fit of the data to eq 3, to where A is the peak area, A_{int} is the intercept found from calibration, and A_0 is the peak area at the solution surface. Six terms were required to fit the data properly ($\nu_{\text{max}} = 6$).

$$A(z, t) - A_{\text{int}} = A_0 \left\{ 1 - \frac{4}{\pi} \sum_{\nu=0}^{\nu=6} \frac{1}{2\nu+1} \sin \frac{(2\nu+1)\pi z}{2L} \times \exp \left[- \left(\frac{(2\nu+1)\pi}{2L} \right)^2 D t \right] \right\} \quad (3)$$

In fitting the data, the probe depth, z , and the solution thickness, L , were held at the measured values. A nonlinear weighted regression was performed to determine the values of the diffusion coefficient, D , and A_0 from provided initial guesses. For the CH₃OH–H₂O and the 39.2–79.3 wt % H₂SO₄ solutions, the diffusion coefficient was determined by using data containing up to 5 mol % total methyl species (CH₃OH, CH₃OH₂⁺, and MHS) based upon Raman intensity–concentration calibration curves. These data correspond up to the first three hours of collection. For the CH₃OH–96.5 wt % H₂SO₄ experiments, spectra corresponding to up to 12 mol % MHS were used (Supporting Information). These data correspond to up to the first four hours of collection.

Results and Discussion

To date, only a few reports of measured diffusion coefficients for atmospherically relevant species in sulfuric acid solutions are available in the literature.^{1,14,15} These coefficients are necessary to understand the processing of atmospherically relevant chemical species by aerosols. In this article, we focus

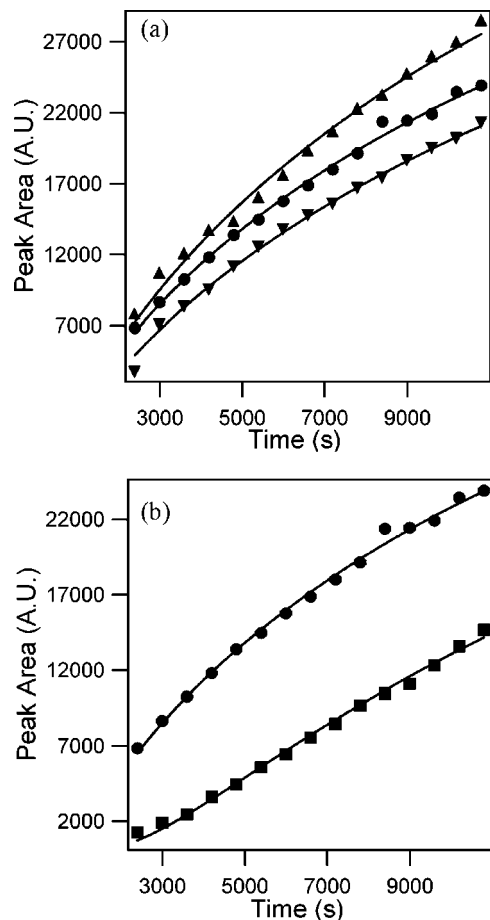


Figure 2. (a) Uptake of CH₃OH into H₂O, following the increases in peak area as a function of time of the CH₃OH CH₃ asymmetric stretch (▲), the CH₃OH C–O stretch (●), and the CH₃OH CH₃ symmetric stretch (▼) at a probe depth of 0.35 cm. (b) Uptake of CH₃OH into H₂O, following the increases in peak area as a function of time for the CH₃OH CO stretch monitored at probe depths of 0.35 cm (●) and 0.57 cm (■).

on estimating the effective diffusion coefficient of CH₃OH in sulfuric acid solutions.

Diffusion Coefficient of CH₃OH into Water. Before determining the diffusion coefficients of CH₃OH into H₂SO₄ solutions, we validated our measurement and analysis methods by measuring the diffusion coefficient for CH₃OH into water, a value that is well reported in the literature.^{25–30} In this work, the diffusion was monitored at two different probe depths and using three different vibrational modes. The peak intensity vs time data using ν CO-ss, ν CH₃-as, and ν CH₃-ss are shown in Figure 2a for a 0.35-cm probe depth, and the ν C–O peak intensity vs time data are shown in Figure 2b for both 0.35- and 0.57-cm probe depths. At a fixed probe depth, the three curves in Figure 2a are reasonably parallel with the CH₃-ss/CO ratio equal to ~ 0.8 and the CH₃-as/CO ratio equal to ~ 1.2 . This is expected since all three curves correspond to the same diffusing species and should only differ by fixed calibration constants. Likewise, the position resolved data exhibit the expected time lag that stems from the increased distance of the observation point to the surface.

The solution to Fick's law used here assumes a diffusion coefficient that is independent of concentration. Other experimental methods showed that the diffusion coefficient of methanol in water decreases to a minimum value as the concentration increases from the infinite dilution limit to 25% mol fraction CH₃OH.^{25,27,29} Indeed, when we fit the entire

TABLE 1: Measured and Estimated Diffusion Coefficients for CH₃OH into 0–96.5 wt % H₂SO₄ Solutions and the Viscosities of the Different H₂SO₄ Solutions Used in This Study

solution (wt %)	H ₂ O/H ₂ SO ₄	viscosity (η , cP)	estimate of D (cm ² /s) ($\times 10^{-5}$)	measured D (cm ² /s) ($\times 10^{-5}$)
96.5	0.2	22–23 ^{34,35}	0.049	0.15 \pm 0.06
79.3	1.4	18.6 (295 K) ³⁶	0.094	0.11 \pm 0.04
61.6	3.4	6.0 (295 K) ³⁶	0.29	0.3 \pm 0.1
39.2	8.4	2.4 (295 K) ³⁶	0.80	0.19 \pm 0.08
0 (water)	∞	0.890 (298 K)	1.7	1.4 \pm 0.6

data set, up to ~ 10 h of data, we observed significant deviations of the data from these curves at later times. Thus, only data from the first three hours were used to calculate D where we estimate the maximum total methyl species concentration was $< \sim 5$ mol %.

Sources of Error. We identified several sources of error in our experiments. First, during the time required for measuring the diffusion coefficient, some water will evaporate. We can estimate the water loss by determining the amount of water that is removed by N₂ leaving the system assuming that this stream is now saturated with water vapor. At 23 °C, the partial pressure of H₂O vapor above pure liquid H₂O is 0.023 atm. Thus, in 3 h the maximum water loss is roughly 8.3×10^{-2} g. Given a surface area of ~ 20 cm² and a liquid water density of 1 g cm⁻³, this corresponds to a height change of 4×10^{-3} cm. The greatest water loss will occur when measuring the diffusion of methanol into water, because in the CH₃OH–H₂SO₄ diffusion experiments the vapor pressure of water above the solution is lower by at least a factor of 2.³¹

Second, the choice of peak may also affect the final value of the diffusion coefficient somewhat. Ideally, the monitored peak is free of interference from other vibrational modes. This is the case for the CO stretch at 1020 cm⁻¹. However, D was also determined using the CH₃ symmetric and asymmetric modes centered at 2850 and 2954 cm⁻¹, respectively. There is overlap between modes in the CH stretching region, and therefore, there is more uncertainty associated with the peak areas in this region. The value of D using the CO stretch is $(1.41 \pm 0.04) \times 10^{-5}$ cm²/s, and that using the symmetric and asymmetric stretches is $(1.3 \pm 0.2) \times 10^{-5}$ cm²/s. Thus, there is a much greater uncertainty associated with D when the CH stretching peaks are used, and the values appear to be somewhat lower although the error bars do overlap.

Finally, there is error in the measured probe depth and the solution height. If the measurement error is 0.05 cm, the error on the solution height is 4%. Recalculating the diffusion coefficient using the upper and lower limits for the solution height (1.25 and 1.15 cm, respectively) results in up to 5% difference in the values obtained for D . The measured error on the standard probe depth (0.35 ± 0.05 cm) is 15%, and changing the value of the probe depth by this amount changes D by up to 40%. Clearly, our ability to measure the probe position relative to the liquid surface is the largest systematic source of error in the reported diffusion coefficient, although the variability between the diffusion experiments was less than 40%. The error bars reported in Table 1 are, therefore, set at 40% of the determined diffusion coefficient.

To compare the value D found here with the values found in the literature^{25–30} that were obtained at different temperatures, we plotted the diffusion coefficients for CH₃OH into H₂O as a function of temperature in Figure 3. From the graph, the value obtained in this study is quite consistent with previous measurements.

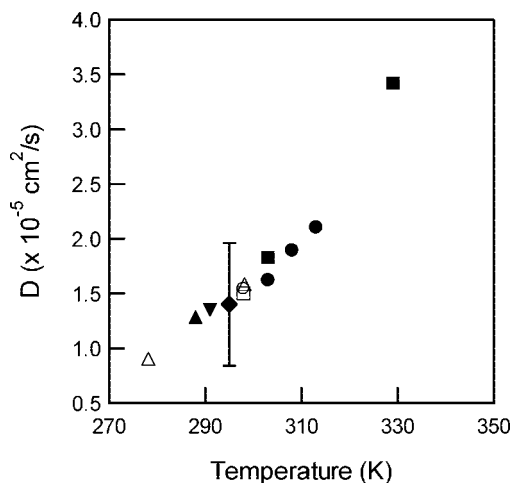


Figure 3. Diffusion coefficients for methanol into water as a function of temperature. The symbols correspond to data from the following references: (▼) Jost,²² (△) Derlacki et al.,²⁵ (○) Hao and Least,²⁶ (●) Lee and Li,²⁷ (■) Mathews and Akgerman,²⁸ (□) Price et al.,²⁹ and (▲) Reid et al.³⁰ (◆) is D measured in this work.

Diffusion of Methanol into Sulfuric Acid Solutions. Experiments were then conducted to follow the diffusion of the methyl species into 39.2 to 96.5 wt % H₂SO₄ solutions. The peak areas vs time data are presented in Figure 4, and the values obtained for D are summarized in Table 1. The effective diffusion coefficients range from $(0.1$ to $0.3) \times 10^{-5}$ cm²/s, values that are up to a factor of 10 smaller than the diffusion coefficient of CH₃OH into H₂O (1.4×10^{-5} cm²/s). The quoted errors correspond to $\pm 40\%$ and are largely due to the uncertainty in the probe depth. The effective diffusion coefficients do not vary systematically with composition, and there appears to be a maximum in D that corresponds to diffusion into 61.6 wt % H₂SO₄ solution. Examining Figure 4b–d where concentrations were monitored using the same CH₃ symmetric stretch, at a fixed time point, for example, $t = 10\,000$ s, confirms that diffusion is 1.5–2 times more rapid at the intermediate concentration (61.6%) than in the other two cases.

As noted in the Introduction, despite the atmospheric relevance, there are very few measured diffusion coefficients in systems where sulfuric acid is the solvent. Instead, D is often estimated using an approach such as the Wilke–Chang method,³⁰ where the dependence of the diffusion coefficient on temperature T and solvent viscosity η is given by^{14,32,33}

$$D = \frac{CT}{\eta} \quad (4)$$

In eq 4, and expanded in eq 5, C is a constant that depends on the molecular weight of the solvent M_B , the association factor used to account for solute–solvent interactions ϕ , and the molar volume of the solute V_A .

$$C = \frac{(7.4 \times 10^{-8})(\phi M_B)^{\frac{1}{2}}}{V_A^{0.6}} \quad (5)$$

For the diffusion of a number of solutes ranging from HCl to DMSO₂ into H₂SO₄ solutions ranging from 30–72 wt %, Klassen et al.¹⁴ found that ϕ is constant and that $\kappa = \phi^* M_B = 64$. This is the value we use for all of our H₂SO₄ concentrations including, for lack of other information, our highest H₂SO₄ concentration. The viscosities, η , of H₂O and 96.5 wt % H₂SO₄ are known,^{34,35} and the viscosities of the 39.2, 61.6, and 79.3 wt % H₂SO₄ solutions required by eq 4 were calculated using

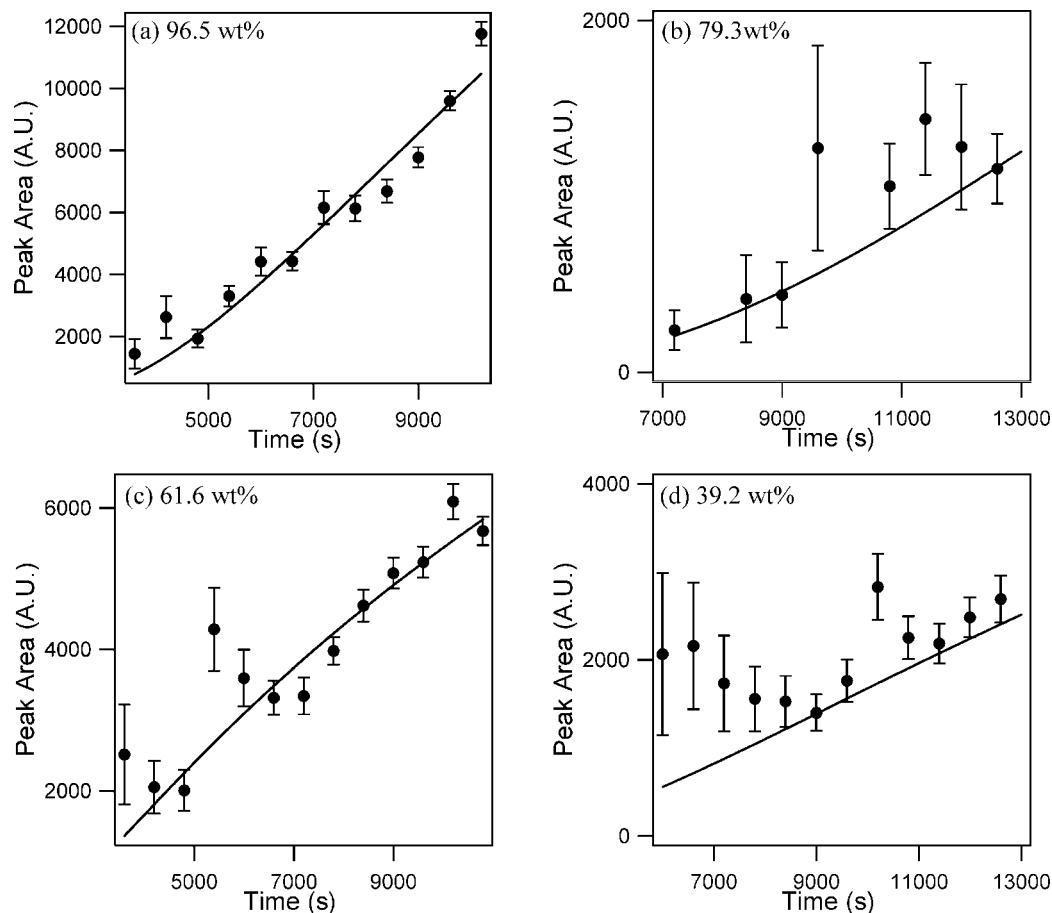


Figure 4. Diffusion of the total methyl species (CH_3OH , CH_3OH_2^+ , and MHS) into 39.2–96.5 wt % H_2SO_4 solutions, following the increases in peak area as a function of time of (a) the O–S–O symmetric stretch and (b–d) the CH_3 symmetric stretch.

TABLE 2: Calculated Distribution of Methyl Species (Percent of CH_3OH , CH_3OH_2^+ , and MHS) in 0–96.5 wt % H_2SO_4 Solutions

wt % H_2SO_4	CH_3OH	CH_3OH_2^+	MHS
96.5			~100
79.3	36.2	43.0	20.8
61.6	57.7	22.9	19.3
39.2	85.5	8.5	6.0
0	100		

eq 1 in ref 36. The viscosities of all the solutions are summarized in Table 1. Values of V_A used in eq 5 were calculated using LeBas additivity with the percent of CH_3OH , CH_3OH_2^+ , and MHS found in Table 2. The molar volume of CH_3OH_2^+ was assumed to be equal to that of CH_3OH , $37 \text{ cm}^3/\text{mol}$.³² The molar volume of MHS was calculated by assuming the density of MHS is equal to that of dimethyl sulfate, $1.33 \text{ g}/\text{cm}^3$.

Before we compare our data to the predictions of eq 4, we must account for the fact that in our experiments methanol is protonated by H_2SO_4 to form CH_3OH_2^+ and can react with H_2SO_4 to form MHS.^{32,33,37,38} In water, the methanol is present as CH_3OH only, whereas in 96.5 wt % H_2SO_4 the conversion to MHS is $(95 \pm 5)\%$.³⁸ On the basis of previous work,²⁰ the protonation to form CH_3OH_2^+ and the reaction to form MHS occur at the air–liquid interface is less than 60 s. This is a time scale shorter than our detection method can measure. Thus, our experiment measures the diffusion coefficient of MHS into 96.5 wt % H_2SO_4 , and the effective diffusion coefficient of three species, CH_3OH , CH_3OH_2^+ , and MHS, into the 39.2 to 79.3 wt % H_2SO_4 solutions. Table 2 summarizes the change in the speciation as a function of the H_2SO_4 concentration that we

determined using a $\text{p}K_{\text{BH}^+}$ of -2.05 ³⁹ with the acidity functions measured for alcohols, H_{ROH} .⁴⁰ The equilibrium constants used are based on those found in the literature.³⁷ Previous work²⁰ studying the uptake of CH_3OH at the surface of and into H_2SO_4 solutions showed a blue shift in peak positions with increasing wt % H_2SO_4 , indicating that the methyl species change with H_2SO_4 concentration.

Despite the complexity of the problem, the Wilke–Chang equation predicts diffusion coefficients close to those observed at 0, 61.6, and 79.3 wt % H_2SO_4 . At the lower H_2SO_4 concentration of 39.2%, the prediction is close to a factor of 3 higher, while at the highest concentration, 96.5%, the prediction is a factor of 2 lower. For the 39.2% and 96.5% sulfuric acid solutions, the Wilke–Chang equation over- and underpredicts, respectively. However, for the pure water case, the 61.6% and 79.3% sulfuric acid solutions, the Wilke–Chang equation is consistent with our observed results. It is not completely clear what solution properties are driving the inconsistency with the two different solutions, 39.2% and 96.5%.

Others have also observed deviations from the Wilke–Chang method for viscous solvents.³⁰ For example, the diffusion coefficients for CO_2 into various solvents remained nearly constant for a range of viscosities (1–27 cP). In contrast, but a study by Kleno et al.¹ using a pulsed gradient spin–echo NMR technique did find that the diffusion coefficients of dimethyl sulfoxide and dimethyl sulfone decreased with increasing H_2SO_4 concentration, as predicted by eq 4.

The speciation of sulfuric acid in the different solutions may also be affecting the observed diffusion of the methanol species.

In H₂SO₄ solutions greater than 80 wt %, ionization is suppressed because of insufficient water⁴¹ and the dominant species is H₂SO₄. Therefore, the 96.5 wt % H₂SO₄ solution is uncharged (or only very weakly charged) and molecular interactions will be weak (van der Waals interactions).⁴¹ Below 80 wt % H₂SO₄, H₂SO₄ is fully dissociated into (H₃O⁺)(HSO₄⁻)⁴² and ionic interactions become important.⁴¹ On the basis of the second dissociation constants for the three different H₂SO₄ solutions,^{42,43} HSO₄⁻ will be further dissociated to (H₃O⁺)(SO₄²⁻). In 39.2 wt % H₂SO₄, 40% of the sulfate species are SO₄²⁻, whereas in 79.3 wt % H₂SO₄, ~9% of the sulfate species are present as SO₄²⁻. (These values are higher than would be expected simply using the dissociation constant of 10⁻² since the activities for HSO₄⁻, SO₄²⁻, and H₂O must be considered.)⁴² The different sulfate species may interact differently with the different methyl species diffusing into the solutions. Referring to Table 2, methanol is present as uncharged (CH₃OH, MHS) and charged (CH₃OH₂⁺ and possibly MHS⁻) species. The interactions between the charged species and the H₂SO₄ solutions may be different from that between the neutral species and the H₂SO₄ solutions. Clearly, more work needs to be done to understand these systems. From our results, it appears that estimations of *D* based solely on the viscosity of the solvent work well for intermediate weight percent sulfuric acid solutions, but are not accurate at the low and high range of concentrations studied here. Protonation, reaction, and the resulting intermolecular forces in acidic solutions are likely key factors in the ability to accurately predict diffusion coefficients.

Conclusions

Raman spectroscopy offers a straightforward method for obtaining diffusion coefficients critical for understanding the chemical processing of volatile organic compounds by atmospheric aerosols in the upper troposphere and lower stratosphere. A diffusion coefficient of $(1.4 \pm 0.6) \times 10^{-5}$ cm²/s at 23 °C was obtained for methanol into water, in agreement with values found in the literature. Values for *D* were also measured for 39.2, 61.6, 79.3, and 96.5 wt % H₂SO₄ solutions. For the 39.2% and 96.5% solutions, the diffusion coefficients do not appear to depend on the viscosity of the H₂SO₄ solutions in an obvious way, indicating that speciation of both methanol and sulfuric acid may be important. This result may be important for uptake studies of organics into acidic solutions that rely on empirically calculated diffusion coefficients.

Acknowledgment. We greatly acknowledge the National Science Foundation for financial support (NSF-CAREER CHE-0134131 (H.C.A.) and CHE-0518042 (B.E.W.)).

Supporting Information Available: Calibration curves used to determine the mol % methyl species (CH₃OH, CH₃OH₂⁺, MHS)—area relationships. This material is available free of charge via the Internet at <http://pubs.acs.org>.

References and Notes

- (1) Kleno, J. G.; Kristiansen, M. W.; Nielsen, C. J.; Pederson, E. J.; Williams, L. R.; Pederson, T. *J. Phys. Chem. A* **2001**, *105*, 8440–8444.
- (2) Curtius, J.; Sierau, B.; Arnold, F.; de Reus, M.; Strom, J.; Scheeren, H. A.; Lelieveld, J. *J. Geophys. Res.* **2001**, *106*, 31975–31990.
- (3) Andronache, C.; Chameides, W. L.; Davis, D. D.; Anderson, B. E.; Poeschel, R. F.; Bandy, A. R.; Thornton, D. C.; Talbot, R. W.; Kasibhatla, P.; Kiang, C. S. *J. Geophys. Res.* **1997**, *102*, 28511–28536.
- (4) Facchini, M. C.; Decesari, S.; Mircea, M.; Fuzzi, S.; Loglio, G. *Atmos. Environ.* **2000**, *34*, 4853–4857.
- (5) Facchini, M. C.; Mircea, M.; Fuzzi, S.; Charlson, R. J. *Nature* **1999**, *401*, 257–259.
- (6) Murphy, D. M.; Thomson, D. S.; Mahoney, M. J. *Science* **1998**, *282*, 1664–1669.
- (7) Galbally, I. E.; Kirstine, W. *J. Atmos. Chem.* **2002**, *43*, 195–229.
- (8) Heikes, B. G.; Chang, W.; Pilson, M. E. Q.; Swift, E.; Singh, H. B.; Guenther, A.; Jacob, D. J.; Field, B. D.; Fall, R.; Riemer, D.; Brand, L. *Global Biogeochem. Cycles* **2002**, *16*, 1133.
- (9) Singh, H.; Chen, Y.; Staudt, A.; Jacob, D.; Blake, D.; Heikes, B.; Snow, J. *Nature* **2001**, *410*, 1078–1081.
- (10) Singh, H. B.; Salas, L. J.; Chatfield, R. B.; Czech, E.; Fried, A.; Walega, J.; Evans, M. J.; Field, B. D.; Jacob, D. J.; Blake, D.; Heikes, B.; Talbot, R.; Sachse, G.; Crawford, J. H.; Avery, M. A.; Sandholm, S.; Fuelberg, H. *J. Geophys. Res.* **2004**, *109*, D15S07.
- (11) Tie, X.; Guenther, A.; Holland, E. *Geophys. Res. Lett.* **2003**, *30*, 1881.
- (12) Marti, J. J.; Weber, R. J.; McMurry, P. H. *J. Geophys. Res.* **1997**, *102*, 6331–6339.
- (13) Wehner, B.; Petaja, T.; Boy, M.; Engler, C.; Birmili, W.; Tuch, T.; Wiedensohler, A.; Kulmala, M. *Geophys. Res. Lett.* **2005**, *32*, L17810.
- (14) Klassen, J. K.; Hu, Z.; Williams, L. R. *J. Geophys. Res.* **1998**, *103*, 16197–16202.
- (15) Langenberg, S.; Proksch, V.; Schurath, U. *Atmos. Environ.* **1998**, *32*, 3129–3137.
- (16) Torn, R. D.; Nathanson, G. M. *J. Phys. Chem. B* **2002**, *106*, 8064.
- (17) Bardow, A.; Goke, V.; Koss, H.-J.; Lucas, K.; Marquardt, W. *Fluid Phase Equilib.* **2005**, *228–229*, 357–366.
- (18) Hilton, M.; Lettington, A. H.; Mills, I. M. *Meas. Sci. Technol.* **1995**, *6*, 1236–1241.
- (19) Rothman, L. S.; Jacquemart, D.; Barbe, A.; Benner, D. C.; Birk, M.; Brown, L. R.; Carleer, M. R., Jr.; Chance, K.; Coudert, L. H.; Dana, V.; Devi, V. M.; Flaud, J.-M.; Gamache, R. R.; Goldman, A.; Hartmann, J.-M.; Jucks, K. W.; Maki, A. G.; Mandin, J.-Y.; Massie, S. T.; Orphal, J.; Perrin, A.; Rinsland, C. P.; Smith, M. A. H.; Tennyson, J.; Tolchenov, R. N.; Toth, R. A.; Auwera, J. V.; Varanasi, P.; Wagner, G. *J. Quant. Spectrosc. Radiat. Transfer* **2005**, *96*, 139–204.
- (20) Van Loon, L. L.; Allen, H. C. *J. Phys. Chem. A* **2008**, *112*, 7873–7880.
- (21) McCreery, R. L. *Raman Spectroscopy for Chemical Analysis*; Wiley & Sons: New York, 2000.
- (22) Jost, W. *Diffusion in Solids, Liquids, Gases*; Academic Press: New York, 1960.
- (23) Jacobs, M. *Diffusion Processes*; Springer-Verlag: New York, 1967.
- (24) Sissom, L. E.; Pitts, D. R. *Elements of Transport Phenomena*; McGraw-Hill: New York, 1972.
- (25) Derlacki, Z. J.; Easteal, A. J.; Edge, A. V. J.; Woolf, L. A. *J. Phys. Chem.* **1985**, *89*, 5318–5322.
- (26) Hao, L.; Leaist, D. G. *J. Chem. Eng. Data* **1996**, *41*, 210–213.
- (27) Lee, Y. E.; Li, S. F. Y. *J. Chem. Eng. Data* **1991**, *36*, 240–243.
- (28) Matthews, M. A.; Akgerman, A. *J. Chem. Eng. Data* **1988**, *33*, 122–123.
- (29) Price, W. S.; Ide, H.; Arata, Y. *J. Phys. Chem. A* **2003**, *107*, 4784–4789.
- (30) Reid, R. C.; Prausnitz, J. M.; Poling, B. E. *The Properties of Gases and Liquids*, 4th ed.; McGraw-Hill: New York, 1987.
- (31) Speight, J. G. *Perry's Standard Tables and Formulas for Chemical Engineers*; McGraw-Hill: New York, 2003.
- (32) Iraci, L. T.; Essin, A. M.; Golden, D. M. *J. Phys. Chem. A* **2002**, *106*, 4054–4060.
- (33) Kane, S. M.; Leu, M.-T. *J. Phys. Chem. A* **2001**, *105*, 1411–1415.
- (34) Viscosity of Liquids. In *CRC Handbook of Chemistry and Physics, Internet Version*, 87th ed.; Lide, D. R., Ed.; Taylor and Francis: Boca Raton, FL, 2007.
- (35) Inorganics. BASF, The Chemical Company. <http://www.inorganics.basf.com/>. Accessed 09-23-08 using keyword search sulfuric acid viscosity.
- (36) Williams, L. R.; Long, F. S. *J. Phys. Chem. A* **1995**, *99*, 3748–3751.
- (37) Deno, N. C.; Newman, M. S. *J. Am. Chem. Soc.* **1950**, *72*, 3852–3856.
- (38) Van Loon, L. L.; Allen, H. C. *J. Phys. Chem. B* **2004**, *108*, 17666–17674.
- (39) Perdoncin, G.; Scorrano, G. *J. Am. Chem. Soc.* **1977**, *99*, 6983–6986.
- (40) Lee, D. G.; Cameron, R. *J. Am. Chem. Soc.* **1971**, *93*, 4724–4728.
- (41) Tomikawa, K.; Kanno, H. *J. Phys. Chem. A* **1998**, *102*, 6082–6088.
- (42) Knopf, D. A.; Luo, B. P.; Krieger, U. K.; Koop, T. *J. Phys. Chem. A* **2003**, *107*, 4322–4332.
- (43) Lund Myhre, C. E.; Christensen, D. H.; Nicolaisen, F. M.; Nielsen, C. J. *J. Phys. Chem. A* **2003**, *107*, 1979–1991.